

# Poloidal Magnetic Fields In Superconducting Neutron Stars

K. T. Henriksson<sup>\*</sup> and I. Wasserman<sup>†‡</sup>

*Center for Radiophysics and Space Research, Cornell University, Ithaca, NY 14853, USA*

9 July 2018

## ABSTRACT

We develop the formalism for computing the magnetic field within an axisymmetric neutron star with a strong Type II superconductor core surrounded by a normal conductor. The formalism takes full account of the constraints imposed by hydrostatic equilibrium with a barotropic equation of state. A characteristic of this problem is that the currents and fields need to be determined simultaneously and self-consistently. Within the core, the strong Type II limit  $B \ll H$  allows us to compute the shapes of individual field lines. We specialize to purely poloidal magnetic fields that are perpendicular to the equator, and develop the “most dipolar case” in which field lines are vertical at the outer radius of the core, which leads to a magnetic field at the stellar surface that is as close to a dipole as possible. We demonstrate that although field lines from the core may only penetrate a short distance into the normal shell, boundary conditions at the inner radius of the normal shell control the field strength on the surface. Remarkably, we find that for a Newtonian  $N = 1$  polytrope, the surface dipole field strength is  $B_{\text{surf}} \simeq H_b \epsilon_b / 3$  where  $H_b$  is the magnetic field strength at the outer boundary of the Type II core and  $\epsilon_b R$  is the thickness of the normal shell. For reasonable models,  $H_b \approx 10^{14}$  G and  $\epsilon_b \approx 0.1$  so the surface field strength is  $B_{\text{surf}} \simeq 3 \times 10^{12}$  G, comparable to the field strengths of many radiopulsars. In general,  $H_b$  and  $\epsilon_b$  are both determined by the equation of state of nuclear matter and by the mass of the neutron star, but  $B_{\text{surf}} \sim 10^{12}$  G is probably a robust result for the “most dipolar” case. We speculate on how the wide range of neutron star surface fields might arise in situations with less restrictions on the internal field configuration. We show that quadrupolar distortions are  $\sim -10^{-9}(H_b/10^{14} \text{ G})^2$  and arise primarily in the normal shell for  $B \ll H_b$ .

**Key words:** stars: neutron; magnetic fields

## 1 INTRODUCTION

Theoretical arguments predict that the protons in the core of a neutron star form a superconductor (Baym et al. 1969), which will be Type II provided that  $\kappa = 1/k_L \xi_p > 1/\sqrt{2}$ , where  $\xi_p$  is the coherence length and  $1/k_L$  is the London length (Easson & Pethick 1977); numerically

$$\begin{aligned} k_L^2 &= \frac{4\pi n_p e^2}{m_p^* c^2} = \frac{4p_{F,p}^3 e^2}{3\pi \hbar^3 m_p^* c^2} = (306 \text{ fm})^{-2} \left( \frac{p_{F,p}}{50 \text{ MeV}} \right)^3 \left( \frac{m_p}{m_p^*} \right) \\ \xi_p &= \frac{\hbar p_{F,p}}{\pi \Delta_p m_p^*} = \frac{3.33 \text{ fm} (p_{F,p}/50 \text{ MeV})}{\Delta_p (\text{MeV}) (m_p^*/m_p)} \\ \kappa &= \frac{1}{k_L \xi_p} = \frac{91.8 \Delta_p (\text{MeV}) (m_p^*/m_p)^{3/2}}{(p_{F,p}/50 \text{ MeV})^{5/2}} \end{aligned} \tag{1}$$

where  $m_p^*$  is the proton effective mass (e.g. Andreev & Bashkin 1975; Alpar et al. 1984; Sedrakian & Sedrakian 1995; Zuo 2012). The gap energy in MeV is  $\Delta_p (\text{MeV}) = 0.15 T_{c,p,9}$  for a critical temperature  $T_{c,p} = 10^9 T_{c,p,9}$  K (because the pairing is

<sup>\*</sup> Email: kth48@cornell.edu

<sup>†</sup> Email: ira@astro.cornell.edu

<sup>‡</sup> Corresponding Author

$^1S_0$ ) and  $n_p = p_{F,p}^3/3\pi^2\hbar^3$  is the proton density. We expect  $p_{F,p} \simeq 50$  MeV at or just below nuclear density,  $n_{\text{nuc}} = 0.16 \text{ fm}^{-3}$ , which is near the boundary between the superconducting core and normal conducting crust inside a neutron star (Baym et al. 1971; Haensel 2001) Although calculations of  $\Delta_p$  are still being refined (Zuo et al. 2008, 2004), Eq. (1) is likely to be consistent with Type II superconductivity for  $n_b \lesssim 2n_{\text{nuc}}$ .

Two recent observations are relevant to this question. First, X-ray observations of the Cassiopeia A neutron star are consistent with cooling via the Cooper pair formation process (Flowers et al. 1976; Shternin et al. 2011; Page et al. 2011), and require proton superconductivity to suppress the contribution from URCA processes, particularly Modified URCA; if  $T_{c,p,9} \gtrsim 2 - 3$  throughout the Cassiopeia A neutron star, these processes are unimportant (Shternin et al. 2011). Second, the discovery of a  $2M_\odot$  neutron star favors relatively stiff equations of state of nuclear matter, in which case internal densities may not be far above  $n_{\text{nuc}}$  (Demorest et al. 2010). We can quantify using relativistic polytropes, where the relationship between pressure  $P$  and baryon density  $n_b$  is  $P \propto n_b^{1+1/N}$ ; to fix the scale we use the chemical potential is  $\mu_{\text{nuc}} = m_b(1 + \epsilon_{\text{nuc}})$  at nuclear density, where  $m_b$  is the baryon mass. Requiring (i)  $\epsilon_{\text{nuc}} = 0.065$ , a reasonable value (Hebel et al. 2007), (ii)  $M_{\text{max}} > 2M_\odot$  and (iii) sound speed  $< 1$  implies  $0.54 \leq N \leq 0.73$ , for which  $M_{\text{max}} \approx 5.44(\epsilon_{\text{nuc}})^{N/2}M_\odot \simeq 2.0 - 2.6M_\odot$ , and central densities are  $n_b/n_{\text{nuc}} \simeq 1.7 - 2.4$  and  $n_b/n_{\text{nuc}} \simeq 2.4 - 6.7$  for  $M = 1.4M_\odot$  and  $M = 2.0M_\odot$ , respectively. Actual equations of state may be stiffer than  $N = 1$  in some density ranges, and softer in others, but central densities may not be much larger than  $\simeq 2n_{\text{nuc}}$  for “typical” neutron stars. In this relatively limited density range, and with  $T_{c,p,9} \gtrsim 2 - 3$ ,  $\kappa > 1/\sqrt{2}$  is likely to be true, so the superconductor is Type II.

Inside a Type II superconductor, magnetic flux is concentrated within flux tubes, each of which carries magnetic flux  $\Phi_0 = \pi\hbar c/e \approx 2.06 \times 10^{-7} \text{ G cm}^2$ . The spacing between flux tubes in a triangular lattice is  $\ell_B = (2\Phi_0/B\sqrt{3})^{1/2} = 4880B_{12}^{-1/2} \text{ fm}$ , where  $B = 10^{12}B_{12} \text{ G}$  is the magnitude of the magnetic induction in the core; consequently

$$k_L\ell_B = 15.9B_{12}^{-1/2} \left( \frac{p_{F,p}}{50 \text{ MeV}} \right)^{3/2} \left( \frac{m_p}{m_p^*} \right)^{1/2}. \quad (2)$$

When  $k_L\ell_B \gg 1$ , the magnetic field is confined to flux tubes that do not interact with one another to a first approximation; the local magnetic field near a flux tube decays exponentially with a scale length  $1/k_L$ . Under these circumstances, the magnetic free energy is nearly proportional to  $B$  and the magnetic field strength inside the superconductor is approximately (Easson & Pethick 1977)

$$H \simeq H_{c1} \simeq \frac{\Phi_0 k_L^2 \ln \kappa}{4\pi} = \frac{p_{F,p}^3 e \ln \kappa}{3\pi m_p^* c \hbar^2} = 8.75 \times 10^{13} \text{ G} \left( \frac{\ln \kappa}{5} \right) \left( \frac{p_{F,p}}{50 \text{ MeV}} \right)^3 \left( \frac{m_p}{m_p^*} \right) \quad (3)$$

which is a function of density, since  $p_{F,p}$ ,  $m_p^*$  and  $\kappa$  vary with density according to the neutron star equation of state; from the calculations in Zuo et al. (2008), we conclude that a fairly good approximation is  $H \propto \rho^b$  with  $b \approx 1.6 - 1.8$ . Since  $k_L\ell_B$  is large, the superconducting core of a neutron star is in the “strong Type II” regime. That the magnetic field strength in this regime is fixed by the density both simplifies and complicates the computation of magnetic structure. The strong Type II limit fails within a (presumably thin) transition region within which protons cluster progressively into nuclei until the superconducting free proton fluid disappears entirely. The outer shell of the neutron star is then a normal conductor.

The challenge is to compute the magnetic field structure including both Type II inner core and normal outer shell, which then matches to the (vacuum) exterior. In this paper, we focus on the “most dipolar” external fields within stars we model as  $N = 1$  Newtonian polytropes. In order to find these most dipolar configurations, we require that field lines exit the core vertically. We then show that if  $H_b \gg B$  is the magnetic field strength at the outer edge of the Type II core, then the magnetic field at the base of the normal shell is very nearly  $-\hat{\theta}H_b \sin \theta$ , provided that the transition region between the core and normal shell is thin enough. This boundary condition is consistent with a particular dipole field solution within the normal shell. From this solution we find that the characteristic magnetic dipole field strength at the stellar surface under these conditions is approximately

$$\frac{\mu}{R^3} \simeq \frac{H_b \epsilon_b}{3} \simeq 2.91 \times 10^{12} \text{ G} \left( \frac{\ln \kappa}{5} \right) \left( \frac{p_{F,p}}{50 \text{ MeV}} \right)^3 \left( \frac{m_p}{m_p^*} \right) \left( \frac{\epsilon_b}{0.1} \right). \quad (4)$$

where the thickness of the crust is  $\epsilon_b R$  and  $\mu$  is the dipole moment.

Eq. (4) is one of the central results of this paper: it relates the dipole magnetic field strength directly to the magnetic field in the Type II core and the thickness of the stellar crust, both of which may be computed given the nuclear equation of state. Although Eq. (4) depends sensitively on  $p_{F,p}$  at the boundary of the Type II core, it is noteworthy that the implied field strength in this model is comparable to  $B \sim 10^{12} \text{ G}$ , which is characteristic of many pulsars and accreting neutron stars. Detailed results will differ among equations of state; in particular,  $\epsilon_b \propto \rho_b^{1/N}$ , where  $\rho_b$  is the density at the base of the normal shell, for a polytrope of index  $N$ .

Other calculations based on magneto-thermal effects and evolution have also arrived at surface magnetic field strengths of order  $10^{12} - 10^{13} \text{ G}$  (Blandford et al. 1983; Pons et al. 2009). These arguments did not consider the Type II core, and the significant boundary condition it imposes at the base of the neutron star’s normal outer shell.

In §2 we present a general overview of the problem we address here. In this section, we derive (i) the implications of hydrostatic balance for magnetic field configurations, (ii) the equations that we solve in the Type II core, (iii) the equations that hold in the normal shell, and (iv) the formalism for computing stellar distortions. We give specific results relevant to the “most dipolar” case and derive, in particular, Eq. (4), but also highlight causes of perturbations around this simple solution.

In §3 we illustrate some of the salient features of the problem via a toy model that is totally analytic and surprisingly close to being realistic. Then in §4 we present particular results for the most dipolar case of greatest interest. In this section, we consider not only the simplest version of the “most dipolar” case but also perturbations around that solution that lead to non-dipolar corrections to the fields. We conclude in §5 by reviewing these solutions and suggesting extensions to other cases that may allow surface field strengths that are either appreciably lower or higher than Eq. (4).

## 2 OVERVIEW

In this paper, we compute the magnetic field for a star with a superconducting core that matches onto a normal crust surrounded by vacuum. We model the star as a Newtonian  $N = 1$  polytrope with a poloidal magnetic field that only distorts the star slightly. Previous calculations of this type were done for poloidal fields of a uniform density star (Roberts 1981) and for toroidal magnetic fields in a Newtonian  $N = 1$  polytrope (Akgün & Wasserman 2008; Akgün 2007; Lander et al. 2012). These two different previous calculations were simpler than those presented here. A significant complication in finding the magnetic field structure is that  $H$  is density-dependent according to Eq. (3); accommodating this complication will require a generalization of the method of solution for a uniform density star (Roberts 1981). Calculations for a toroidal field could account for the density dependence of  $H$  because it was unnecessary to determine the field line shapes, which were specified *a priori* (Akgün & Wasserman 2008).

Our calculations are perturbative in that we assume that the distortions induced by magnetic stresses (which we compute) are small. However, we take full account of the requirements of hydrostatic balance, which constrain the field shapes, just as for normal conductors (Wentzel 1961; Prendergast 1956); our calculations are analogous to those done previously for small magnetic distortions in a normal conductor (Monaghan 1965). We find the “true equilibrium” configurations in which the magnetic distortions are assumed to obey the same equation of state as the unperturbed star. The actual magnetic fields in neutron stars may not be true equilibria in this sense (Mastrano et al. 2011) even though, on sufficiently long time scales, the fields should relax to these states naturally. Even in non-equilibrium field configurations the field at the base of the normal shell will have to match properly to the field in the Type II core. We therefore expect a version of Eq. (4) to remain true for substantially dipolar fields even for configurations that are not true equilibria.

We focus on the “most dipolar” field configurations that arise when field lines hit the outer edge of the Type II core vertically. As we shall see, this is a special configuration, and infinitely many others are possible.

Throughout this paper, we assume that the entire core of the star is superconducting. We argued above that this may be reasonable if the density range in the core is not too large. We expect that the external dipole field that emerges from our “most dipolar” solutions would not be affected significantly if the very inner core of the neutron star is not superconducting.

### 2.1 Requirements of Hydrostatic Balance

The magnetic free energy is  $f(\rho, \mathbf{B})$ , where  $\rho$  is mass density and  $\mathbf{B}$  is magnetic induction; then the magnetic field is  $\mathbf{H} = 4\pi\partial f/\partial\mathbf{B}$ , and the magnetic force density is

$$\mathbf{f}^{mag} = -\rho\nabla\left(\frac{\partial f}{\partial\rho}\right) + \frac{(\nabla\times\mathbf{H})\times\mathbf{B}}{4\pi} = -\rho\nabla\left(\frac{\partial f}{\partial\rho}\right) + \frac{\mathbf{J}\times\mathbf{B}}{c} \quad (5)$$

using Ampère’s law,  $\nabla\times\mathbf{H} = 4\pi\mathbf{J}/c$ . Eq. (5) was derived in Akgün & Wasserman (2008) by taking the divergence of the magnetic stress tensor for a Type II superconductor given by Easson & Pethick (1977); it may also be derived by considering the variation of magnetic energy resulting from small fluid displacements. The equation of hydrostatic balance including pressure, gravity and magnetic forces is

$$0 = -\frac{\nabla P}{\rho} - \nabla\Psi + \frac{\mathbf{f}^{mag}}{\rho} \quad (6)$$

where  $\Psi$  is the gravitational potential,  $P$  is the pressure and  $\rho$  is the mass density. For a barotropic fluid  $P = P(\rho)$  and  $dh(\rho) = dP(\rho)/\rho$ , in which case

$$0 = -\nabla\left(h + \Psi + \frac{\partial f}{\partial\rho}\right) + \frac{\mathbf{J}\times\mathbf{B}}{\rho c}. \quad (7)$$

Eq. (7) is only consistent mathematically if  $\mathbf{J}\times\mathbf{B}/\rho c = -\nabla\Phi$ , where  $\Phi$  is some potential. In axisymmetry,

$$\mathbf{B} = \nabla\times\left[\frac{A(r,\theta)\hat{\phi}}{r\sin\theta}\right] + B_T(r,\theta)\hat{\phi} \quad (8)$$

and  $\mathbf{H} = \mathbf{H}_P + H_T\hat{\phi}$ ; the current density is

$$\nabla\times\mathbf{H} = \nabla\times\mathbf{H}_P + \frac{\nabla(H_T r\sin\theta)\times\hat{\phi}}{r\sin\theta} \equiv \frac{4\pi\mathbf{J}\hat{\phi}}{c} + \frac{\nabla(H_T r\sin\theta)\times\hat{\phi}}{r\sin\theta}. \quad (9)$$

Requiring that  $\hat{\phi}\cdot(\mathbf{J}\times\mathbf{B}) = 0$  implies that  $H_T r\sin\theta = \mathcal{H}_T(A)$ ; the Lorentz acceleration  $\mathbf{J}\times\mathbf{B}/\rho c$  is a total gradient if

$$J - \frac{cB_T}{4\pi} \frac{d\mathcal{H}_T(A)}{dA} = c\rho r \sin \theta \mathcal{J}(A) \quad (10)$$

which means that  $-\nabla\Phi = \mathcal{J}(A)\nabla A$ . Eq. (10) is well-known for normal magnetic equilibria (Prendergast 1956; Woltjer 1960; Wentzel 1961; Monaghan 1965); the  $B_T = 0$  version of Eq. (10) has also been derived previously for Type II superconductors with poloidal fields (Roberts 1981; Akgün 2007). Similar results have been derived independently by Lander (2013).

We are interested in poloidal fields only, so  $B_T = 0$ . (See also Lander 2013, for specific models including poloidal and toroidal fields.) We also assume that  $f(\rho, \mathbf{B}) = f(\rho, B)$  i.e. there are no preferred directions in space so the free energy only depends on  $B = |\mathbf{B}|$ . In this situation, the magnetic field and magnetic induction are parallel:  $\mathbf{H} = 4\pi\hat{\mathbf{B}}\partial f/\partial B$  where  $\hat{\mathbf{B}} = \mathbf{B}/B$ .

Our goal is to solve

$$\nabla \times \mathbf{H} = \nabla \times (H\hat{\mathbf{B}}) = \nabla H \times \hat{\mathbf{B}} + H\nabla \times \hat{\mathbf{B}} = 4\pi\rho r \sin \theta \mathcal{J}(A)\hat{\phi} \quad (11)$$

throughout the star. We shall strive for solutions without surface currents; in particular, we are interested in solutions in which field lines cross the equator smoothly and vertically. With this goal in mind, we will have to determine *both* the field configuration *and* its source  $\mathcal{J}(A)$  self consistently, within both the Type II core and the normal shell.

## 2.2 Field Configuration in the Type II Core

In the strong Type II limit,  $H = H(\rho)$  in the core, and invoking the assumption that magnetic distortions are small, we can substitute the unperturbed density of the background star,  $\rho(r)$ , so  $H = H(r)$ .

With this simplification, Eq. (11) is a complicated partial differential equation even if we specify  $\mathcal{J}(A)$  somehow, and we shall not attempt to solve it directly. Instead, we extend the procedure first employed by Roberts (1981) for uniform density stars to stars with  $H(r) \neq \text{constant}$ . Since  $B_T = 0$ , Eq. (8) implies that  $\hat{\mathbf{B}} \cdot \nabla A = 0$  i.e.  $A$  is constant along poloidal field lines. This allows us to consider Eq. (11) along individual field lines.

Let us concentrate on a particular field line. Introduce the parametric independent variable  $s$ , the arc length along this field line; position along the field line is  $\mathbf{r}(s)$  and the tangent to the field line is  $\hat{\mathbf{B}}(s) = d\mathbf{r}(s)/ds$ . There are two directions normal to the field line:  $\hat{\phi}$  and a second direction  $\hat{\mathbf{n}}(s)$  which we define to be  $\hat{\mathbf{n}}(s) = \hat{\phi} \times \hat{\mathbf{B}}(s)$ . The field line curvature is  $K(s)$  given by  $K(s)\hat{\mathbf{n}}(s) = d^2\mathbf{r}(s)/ds^2 = \hat{\mathbf{B}}(s) \cdot \nabla \hat{\mathbf{B}}(s)$ . Eq. (11) is then equivalent to

$$\frac{4\pi J}{c} = 4\pi\rho r \sin \theta \mathcal{J}(A) = -\nabla H \cdot \hat{\mathbf{n}} + KH. \quad (12)$$

For uniform  $H$  the first term in Eq. (12) is absent and we recover the equation found by Roberts (1981). In Eq. (12)  $\mathcal{J}(A)$  is simply a constant associated with the field line.

In axisymmetry, we may choose to specify position along a field line by  $r(s)$  and  $\theta(s)$ ; in that case

$$\hat{\mathbf{B}}(s) = \hat{\mathbf{r}} \frac{dr(s)}{ds} + \hat{\boldsymbol{\theta}} r(s) \frac{d\theta(s)}{ds} \equiv \hat{\mathbf{r}} \cos \Lambda(s) + \hat{\boldsymbol{\theta}} \sin \Lambda(s) \quad (13)$$

and therefore

$$\hat{\mathbf{n}}(s) = \hat{\phi} \times \hat{\mathbf{B}}(s) = -\hat{\mathbf{r}} \sin \Lambda(s) + \hat{\boldsymbol{\theta}} \cos \Lambda(s). \quad (14)$$

The field line curvature is

$$K(s) = \frac{d\Lambda}{ds} + \frac{\sin \Lambda}{r}; \quad (15)$$

using Eq. (14) and Eq. (15) in Eq. (12) we find

$$\frac{d\Lambda}{ds} = \frac{4\pi\rho r \sin \theta \mathcal{J}(A)}{H(r)} - \frac{\sin \Lambda}{r} \left( \frac{r}{H} \frac{dH(r)}{dr} + 1 \right). \quad (16)$$

Eq. (16) and Eq. (13) determine the field line shape jointly, given  $\rho(r)$ ,  $H(\rho)$  and a value of  $\mathcal{J}(A)$ .

For our solutions we shall assume an  $N = 1$  polytrope for which  $\rho(r) = \rho(0) \sin x/x$ , with  $x = \pi r/R$ ; we shall also assume  $H \propto \rho^b$ . With these choices, and the definition  $ds = R d\sigma/\pi$ , Eq. (16) becomes

$$\frac{d\Lambda}{d\sigma} = \frac{\hat{\mathcal{J}}(A)x^b \sin \theta}{(\sin x)^b} - \frac{\sin \Lambda}{x} [b(x \cot x - 1) + 1] \quad (17)$$

where

$$\hat{\mathcal{J}}(A) = \frac{4R^2 \rho(0) \mathcal{J}(A)}{\pi H(0)}; \quad (18)$$

the field line shape is found by solving Eq. (17) along with

$$\frac{dx}{d\sigma} = \cos \Lambda \quad x \frac{d\theta}{d\sigma} = \sin \Lambda. \quad (19)$$

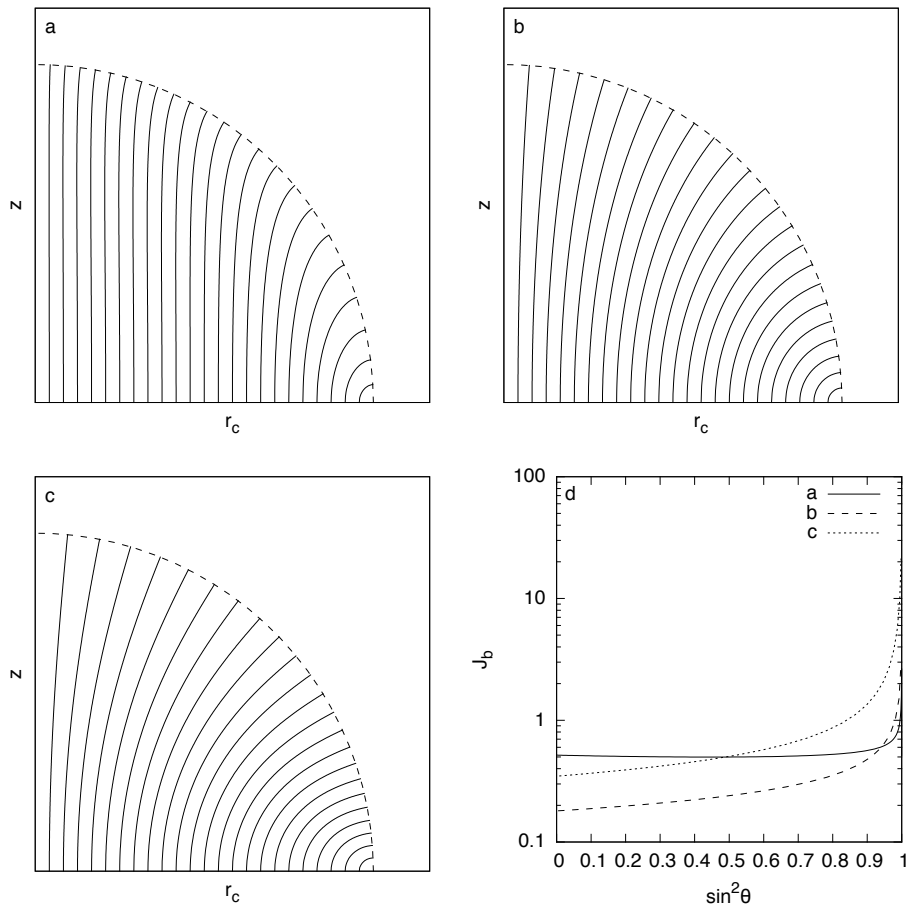


**Figure 1.** Field line configurations in the Type II core for field lines that hit the core boundary radially. Panel a. shows field lines for  $H \propto \rho^{1.6}$  and a  $N = 1$  polytrope density profile; Panel b. shows field lines for uniform  $H$  and  $\rho$ ; Panel c. shows field lines for uniform  $H$  but a  $N = 1$  polytrope density profile. All three models assume that the core radius is  $r_b = 0.9R$ , shown on the plots as a dashed line. Panel d. shows the rescaled current parameter  $\hat{\mathcal{J}}$  for the three models as a function of  $\sin^2 \theta$  on  $r_b$ .

We are interested in solutions that start at some equatorial footpoint where  $x = x(0)$  and  $\theta(0) = \pi/2$ . At this footpoint, symmetry dictates that the field line be perpendicular to the equator; choosing the direction to be vertically upward implies  $\Lambda(0) = -\pi/2$ .

For the “most dipolar” case we also want field lines to hit the outer boundary of the Type II region at  $x = x_b$  with  $\Lambda = -\theta$ . Very generally, it is impossible to find solutions that are exactly vertical throughout the core for a given  $H(\rho)$ . (The solutions are nevertheless close to the toy model developed in §3 that demands that field lines are exactly vertical.) The condition that a field line starts out at  $x(0)$  and  $\theta = \pi/2$  pointing vertically and also hits vertically at  $x_b$  determines the value of  $\hat{\mathcal{J}}(A)$  for that field line. Note that in this context, “ $A$ ” is just a label for the field line; we could just as well label the field line by  $x(0)$ . In fact, this procedure *does not* determine  $A(x, \theta)$  within the Type II core. The end result is  $\hat{\mathcal{J}}(x(0))$  and, since field lines hit  $x_b$  at  $\theta(x(0))$ ,  $\hat{\mathcal{J}}_b(\theta)$  is determined parametrically on the outer boundary of the core.

We can also consider other types of solution for field lines, for instance solutions in which field lines hit  $x_b$  with some other specified set of orientations and, therefore, carry different values of  $\hat{\mathcal{J}}(x(0))$  along with them. We must be careful to choose orientations for which field lines do not cross within the Type II core. But even that restriction allows many different possibilities other than our “most dipolar” case.

As an illustration, Fig. 1 shows the field lines assuming that field lines intersect the outer boundary of the core *radially*. For  $H_b \gg B$ , this is the field configuration needed to match smoothly into regions without currents since  $|B_\theta| \sim |B_r|$  in that case (e.g. Roberts 1981). The current free region may be the normal shell or the vacuum exterior. In order to highlight the effects of variable  $H$  and  $\rho$  inside the core, we show three different cases: (a)  $H \propto \rho^{1.6}$  with a  $N = 1$  polytrope density profile; (b)  $H$  and  $\rho$  uniform, the case considered by Roberts (1981); (c)  $H$  uniform but with a  $N = 1$  polytrope density profile. The lower right panel of Fig. 1 shows  $\hat{\mathcal{J}}_b$  on the boundary of the Type II core, which we placed at  $r_b = 0.9R$ , as a function of  $\sin^2 \theta$ . As can be seen from Fig. 1 the current diverges for field lines near the equator. This is because they start out vertical and must turn through about  $\pi/2$  to hit the boundary radially within the short distance  $r_b - r$ .

The fact that we do not determine  $A(x, \theta)$  in the Type II core means that even with a given set of solutions for individual

field lines, we can consider various “field line densities” within the core. This freedom can accommodate theories of field line evolution in which secular motion of flux tubes leads to different concentrations of flux within the core.

### 2.3 Solution in the Normal Shell

Within the normal shell, it is most straightforward to solve Eq. (11) directly: using  $\mathbf{H} = \mathbf{B}$  and substituting for the poloidal field we get

$$-\frac{H(0)R^2}{\pi^2}[\hat{\mathcal{J}}(A)x \sin x \sin^2 \theta] = \frac{\partial^2 A}{\partial x^2} + \frac{1}{x^2} \left( \frac{\partial^2 A}{\partial \theta^2} - \cot \theta \frac{\partial A}{\partial \theta} \right), \quad (20)$$

where we have used the same parametrization as in Eq. (18) and specialized to the  $N = 1$  polytrope density profile. Eq. (20) would be straightforward to solve given  $\hat{\mathcal{J}}(A)$ . However, we have to determine  $\hat{\mathcal{J}}(A)$  to be consistent with matching conditions at both the inner boundary of the normal shell at  $x_b$  and at the stellar surface, where the field must match smoothly to vacuum.

Matching to a vacuum exterior is accomplished most easily by introducing the expansion

$$A(x, \theta) = \sin \theta \sum_{j=0}^{\infty} A_j(x) P_{2j+1}^1(\cos \theta) \quad (21)$$

where  $P_{2j+1}^1(\mu)$  is an associated Legendre polynomial. Using Eq. (21) in Eq. (20) implies

$$\frac{d^2 A_j(x)}{dx^2} - \frac{(2j+2)(2j+1)A_j(x)}{x^2} = -\frac{H(0)R^2 x \sin x}{\pi^2 N_j} \int_{-1}^{+1} d\mu \sqrt{1-\mu^2} P_{2j+1}^1(\mu) \hat{\mathcal{J}}(A) \quad (22)$$

where

$$N_j = \frac{2(2j+2)(2j+1)}{4j+3}. \quad (23)$$

The source term in Eq. (22) generally involves the entire set of  $A_i$ , not just  $i = j$ . But once  $\hat{\mathcal{J}}(A)$  has been determined, the source term is known, and the boundary condition at the surface  $x = \pi$  is

$$\left( \frac{dA_j(x)}{dx} \right)_{\pi} + \frac{(2j+1)A_j(\pi)}{\pi} = 0 \quad (24)$$

for matching to a vacuum field in the exterior.

Matching to the core requires that the normal component of  $\mathbf{B}$  and tangential component of  $\mathbf{H}$  be continuous across the boundary. In the simplest case, the transition zone thickness may be neglected. If  $\Lambda_b(\theta)$  is the value of  $\Lambda$  for a field line hitting  $x_b$  at  $\theta$  and  $B(\theta)$  is the magnitude of the core induction field there, then the matching conditions are ( $\mu = \cos \theta$ )

$$\begin{aligned} \left( \frac{\partial A}{\partial \mu} \right)_b &= -\frac{R^2 x_b^2 B(\theta) \cos \Lambda_b(\theta)}{\pi^2} \\ \left( \frac{\partial A}{\partial x} \right)_b &= -\frac{R^2 x_b H_b \sin \theta \sin \Lambda_b(\theta)}{\pi^2}. \end{aligned} \quad (25)$$

In the strong Type II regime,  $B(\theta) \ll H_b$  and unless  $\Lambda_b(\theta) \lesssim B/H_b$  the field is predominantly tangential at the base of the normal shell. To a first approximation,  $(\partial A/\partial \mu)_b \approx 0$ , which is equivalent to  $A_j(x_b) \approx 0$ , in the strong Type II regime.

Eq. (24) and Eq. (25) impose three conditions on each  $A_j(x)$ , which is one too many. This overdetermination implies constraints on the form of  $\hat{\mathcal{J}}(A)$  within the shell.

In the “most dipolar” case,  $\Lambda_b(\theta) = -\theta$ , and Eq. (25) implies that the field at the inner edge of the normal shell is approximately  $-\hat{\theta} H_b \sin \theta$  in the limit  $B \rightarrow 0$ . In this limit, field lines from the interior do not penetrate into the normal shell but still influence conditions there via Eq. (25). With  $B = 0$ , the field inside the normal shell is precisely dipolar,  $A(x, \theta) = A_0(x) \sin^2 \theta$ , where

$$\begin{aligned} A_0(x) &= \frac{H_b R^2 f(x; x_b)}{3\pi^2} \\ f(x; x_b) &= \frac{x^3 - x_b^3 + 6x \cos x - 6x_b \cos x_b + (3x^2 - 6) \sin x - (3x_b^2 - 6) \sin x_b}{x(1 + \cos x_b)}. \end{aligned} \quad (26)$$

Within the shell, consistency with Eq. (24) and Eq. (25) requires that

$$\hat{\mathcal{J}}(A) = \hat{\mathcal{J}}_{\text{shell}} = \frac{H_b}{H(0)(1 + \cos x_b)} = \frac{(\sin x_b/x_b)^b}{1 + \cos x_b} \quad (27)$$

which is the simplest case showing how the boundary conditions determine  $\hat{\mathcal{J}}(A)$ . The stellar dipole moment is

$$\mu = R A_0(\pi) = \frac{H_b R^3 f(\pi; x_b)}{3\pi^2}; \quad (28)$$

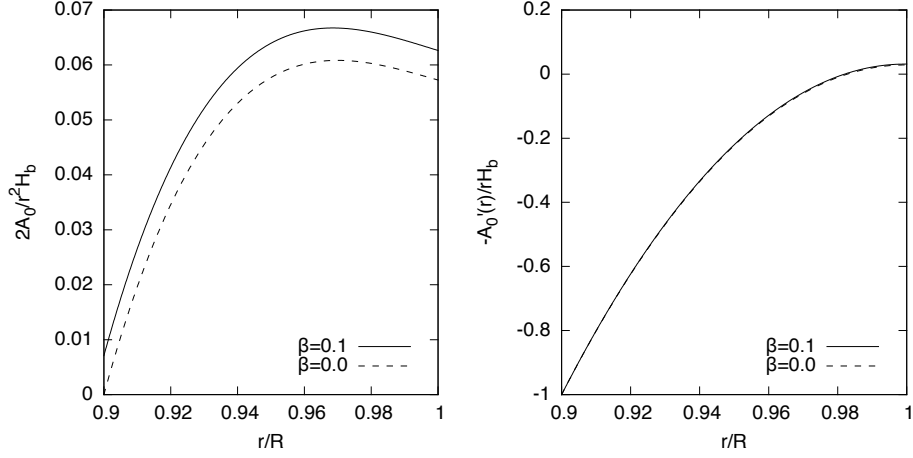


**Figure 2.**  $2A_0/H_b r^2$  (left panel) and  $-(H_b r)^{-1} dA_0/dr$  (right panel) in the normal shell, where  $\mathbf{H} = \mathbf{B} = \hat{\mathbf{r}}(2A_0/r^2) \cos \theta - (r^{-1} dA_0/dr) \hat{\boldsymbol{\theta}} \sin \theta$ . For the functional form of  $A_0$ , see Eq. (31). Two different values of  $B$  are assumed, parameterized by the quantity  $\beta$  defined in Eq. (35); results are shown for  $\beta = 0$  and 0.1.

if  $\pi - x_b \equiv \delta_b = \pi \epsilon_b \ll 1$ ,  $f(\pi; x_b)/3\pi^2 \approx \delta_b/3\pi = \epsilon_b/3$ , which leads to Eq. (4) for thin shells.

Eq. (26) holds when we can neglect the thickness of the transition layer and the radial field that pokes into the normal shell through it. If the transition layer is thin enough, then its effect is to introduce a “surface current” into the jump condition from the Type II core to the normal shell: the tangential field at the base of the normal shell is now

$$B_\theta(x_b, \theta) = -\frac{\pi^2}{R^2 x_b \sin \theta} \left( \frac{\partial A}{\partial x} \right)_b = H_b \sin \Lambda_b(\theta) + \frac{\pi \ell \hat{\mathcal{J}}_b(\theta) H(0) \sin x_b \sin \theta}{R} \quad (29)$$

where  $\ell$  is the thickness of the transition zone. §B contains a brief discussion of the rather complex physics of this region. There, it is shown that Eq. (29) holds as long as field lines do not rotate very much as they pass through the transition zone. Roughly speaking, this will be true provided that  $H_b \ell / BR \ll 1$ ; therefore the second term in Eq. (29) is  $\ll BH(0)/H_b^2$  times the first. Nevertheless, Eq. (29) perturbs the solution away from Eq. (26) even in the “most dipolar” case. In particular, the jump term engenders non-dipolar fields in the shell and outside, and requires a more detailed calculation of  $\hat{\mathcal{J}}(A)$  inside the shell. As long as the corrections to Eq. (26) are small they may be computed perturbatively. A method of calculation is outlined in Appendix A.

Relaxing the  $B \rightarrow 0$  limit also perturbs the solution even if the transition zone thickness is negligible. If we assume that

$$A(x_b, \theta) = \frac{1}{2} B r_b^2 \sin^2 \theta = \frac{B R^2 x_b^2 \sin^2 \theta}{2\pi^2} \quad (30)$$

then the unperturbed field inside the normal shell remains dipolar, and is altered to  $A_0(x, \theta) = A_0(x; B) \sin^2 \theta$ , where

$$A_0(x; B) = \frac{B R^2 x_b^3}{2\pi^2 x} + \frac{(H_b + B/2) R^2 f(x; x_b)}{3\pi^2} \quad (31)$$

and the current density parameter is

$$\hat{\mathcal{J}}_{\text{shell}} = \frac{H_b(1 + B/2H_b)}{H(0)(1 + \cos x_b)}. \quad (32)$$

Eq. (31) implies a magnetic moment

$$\mu(B) = \frac{B r_b^3}{2} + \frac{(H_b + B/2) R^3 f(\pi; x_b)}{3\pi^2} \quad (33)$$

which reduces to Eq. (28) for  $B = 0$ ; the first term in Eq. (33) is simply the dipole moment associated with  $B$  and the second arises from the currents in the normal shell. Fig. 2 shows  $A_0/r^2$  and  $-r^{-1} dA_0/dr$  in the normal shell, where the magnetic field is  $\mathbf{H} = \mathbf{B} = \hat{\mathbf{r}}(2A_0/r^2) \cos \theta - (r^{-1} dA_0/dr) \hat{\boldsymbol{\theta}} \sin \theta$ . In the limit that the transition from superconductor to normal conductor takes place within a region of zero thickness,  $H$  is discontinuous at the boundary between core and shell, but the radial component of  $\mathbf{B}$  and the  $\hat{\boldsymbol{\theta}}$  component of  $\mathbf{H}$  are continuous, as required by Maxwell’s equations with no surface currents. Appendix B outlines how  $\mathbf{H}$  field changes smoothly when the transition region has nonzero thickness. Within the Type II core,  $H = H(\rho)$  is independent of  $\theta$ .

Eq. (31) implies that magnetic field lines from the core enter the shell. The bounding field line entering from the core has  $A = \frac{1}{2} B r_b^2$ , and therefore defines a region  $\theta \leq \theta_{\text{II}}(x)$  where

$$\sin^2 \theta_{\text{II}}(x) = \frac{\beta}{\beta x_b/x + \hat{f}(x; x_b)}; \quad (34)$$

in Eq. (34)

$$\beta \equiv \frac{3\pi^2 B r_b^2}{(2H_b + B)R^2 f(\pi; x_b)} \quad \tilde{f}(x; x_b) \equiv \frac{f(x; x_b)}{f(\pi; x_b)}. \quad (35)$$

The region occupied by the field lines is small if  $\beta \sim B/H_b \epsilon_b \ll 1$ ; note that this is more restrictive than the condition for validity of the strong Type II regime,  $B \ll H_b$ . Eq. (34) indicates that the bounding field line rises from  $\theta = \pi/2$  close to  $x_b$ , remaining at  $\theta \sim 1$  as long as  $\tilde{f}(x; x_b) \sim \beta$ , which is the case for  $x/x_b - 1 \lesssim \beta$ . Ultimately, the bounding field lines emerge at  $x = \pi$  confined to a polar cap with  $\theta \lesssim \sqrt{\beta}$ . The volume of the region occupied by impinging field lines is only  $\sim \beta$  times the volume of the shell. In the limit  $\beta \rightarrow 0$  field lines from the core *do not* penetrate into the normal shell.

However, within that volume,  $\Delta\hat{\mathcal{J}}(A) = \hat{\mathcal{J}}(A) - \hat{\mathcal{J}}_{\text{shell}} \neq 0$  because field lines entering from the core carry their  $\hat{\mathcal{J}}(A)$  along with them. The zeroth order solution represented by Eq. (31) and Eq. (32) requires perturbative corrections driven by the difference  $\Delta\hat{\mathcal{J}}(A)$  within this region; the corrections are  $\mathcal{O}(\beta\Delta\hat{\mathcal{J}}(A)/\hat{\mathcal{J}}_{\text{shell}})$ . Appendix A outlines how these corrections may be taken into account.

## 2.4 Magnetic Distortions Due to Poloidal Fields

For poloidal fields, the Lorentz acceleration is  $-\nabla\Phi = \mathcal{J}(A)\nabla A$ , so

$$\Phi(A) = -\frac{\pi H(0)}{4R^2 \rho(0)} \int_0^A dA' \hat{\mathcal{J}}(A'), \quad (36)$$

and the Bernoulli equation is

$$C = h + \Psi + \frac{\partial f}{\partial \rho} + \Phi \quad (37)$$

where  $C$  is the Bernoulli constant. For perturbations of a  $N = 1$  polytrope, if we expand in Legendre polynomials

$$\Psi(x, \theta) = \sum_l \Psi_l(x) P_l(\cos \theta) \quad (38)$$

we get

$$\frac{1}{x^2} \frac{d}{dx} \left[ x^2 \frac{d\Psi_l(x)}{dx} \right] + \left[ 1 - \frac{l(l+1)}{x^2} \right] \Psi_l(x) = \delta C \delta_{l,0} - \left( \frac{\partial f}{\partial \rho} + \Phi \right)_l \equiv \delta C \delta_{l,0} + M_l(x) \quad (39)$$

where the magnetic potentials are expanded in the same fashion as Eq. (38) and  $\delta C$  is the perturbation of the Bernoulli constant away from its background value. The general solution of Eq. (39) that is regular at  $x = 0$  is

$$\Psi_l(x) = \delta C \delta_{l,0} + j_l(x) \left[ K_l + \int_x^\pi dx' (x')^2 y_l(x') M_l(x') \right] + y_l(x) \int_0^x dx' (x')^2 j_l(x') M_l(x') \quad (40)$$

where  $j_l(x)$  and  $y_l(x)$  are spherical Bessel functions. The constants  $K_0$  and  $\delta C$  are determined by the conditions  $\Psi_0(\pi) = 0 = [d\Psi(x)/dx]_\pi$ , which imply

$$\delta C = K_0 = -\frac{1}{\pi} \int_0^\pi dx x^2 j_0(x) M_0(x), \quad (41)$$

and the constants  $K_l$  are determined by the conditions  $[d\Psi_l(x)/dx]_\pi + (l+1)\Psi_l(\pi)/\pi = 0$ , which imply ( $f'_l(x) \equiv df_l(x)/dx$ )

$$0 = K_l \left[ j'_l(\pi) + \frac{(l+1)j_l(\pi)}{\pi} \right] + \left[ y'_l(\pi) + \frac{(l+1)y_l(\pi)}{\pi} \right] \int_0^\pi dx x^2 j_l(x) M_l(x). \quad (42)$$

For  $l > 0$ ,

$$\Psi_l(\pi) = -\frac{1}{\pi^2 j'_l(\pi) + (l+1)\pi j_l(\pi)} \int_0^\pi dx x^2 j_l(x) M_l(x). \quad (43)$$

We may define the stellar multipole moment by  $\Psi_l(\pi) = -GM\mathcal{M}_l/R$ . With this definition, the contribution to the moment of inertia tensor resulting from the quadrupolar distortion  $\mathcal{M}_2$  is  $\delta\mathbf{I}_2 = -\frac{1}{3}MR^2\mathcal{M}_2(-\hat{x}\hat{x} - \hat{y}\hat{y} + 2\hat{z}\hat{z})$ .

In the ‘‘most dipolar’’ case with negligible transition layer thickness and core magnetic induction, the distortion arises entirely from magnetic stresses inside the crust and is quadrupolar. In this case, ( $\Theta(z) = 1$  for  $z > 0$ , zero otherwise)

$$\mathcal{M}_2(x) = -\frac{H_b^2 f(x; x_b) \Theta(x - x_b)}{18\pi\rho(0)(1 + \cos x_b)} = -\frac{2H_b^2 R^3 f(x; x_b) \Theta(x - x_b)}{9\pi^2 M(1 + \cos x_b)} \quad (44)$$

and ( $\pi^2 j'_2(\pi) + 3\pi j_2(\pi) = \pi$ )

$$\mathcal{M}_2 = -\frac{2H_b^2 R^4}{9\pi^3 GM^2} \int_{x_b}^\pi \frac{dx x^2 j_2(x) f(x; x_b)}{1 + \cos x_b} \equiv -\frac{2H_b^2 R^4 \mathcal{I}(x_b)}{9\pi^3 GM^2}. \quad (45)$$



For thin shells,  $\mathcal{I}(x_b) \approx 9\pi/2 = 14.14$ , independent of the shell thickness; for  $\epsilon_b = 0.1$ , it is  $\mathcal{I}(0.9\pi) = 11.44$ ; consequently

$$\mathcal{M}_2 = -1.39 \times 10^{-9} H_{b,14}^2 R_{10}^4 M_{1.4}^{-2} \left[ \frac{\mathcal{I}(x_b)}{10} \right] \quad (46)$$

where  $H_b = 10^{14} H_{b,14}$  G,  $R = 10R_{10}$  km and  $M = 1.4M_{1.4}M_\odot$ . Thus, the scale of the quadrupolar distortion is determined by the value of  $H_b$  for  $B/H_b \ll 1$ ; for terms  $\mathcal{O}(B)$ , see Eq. (54) and Eq. (55).

### 3 TOY MODEL: VERTICAL FIELD IN THE CORE

We shall be interested in solutions that lead to external fields as close to dipolar as possible; such solutions have fields that are vertical at the outer boundary of the Type II core. In general, these will not allow field lines that are exactly vertical throughout the core.

Nevertheless, to develop a toy model, suppose  $\mathbf{H} = H(r)\hat{\mathbf{z}}$ ; this model will illustrate many features of the problem. For vertical fields,  $\mathcal{J}_{\text{II}}(A) = \text{constant} = \mathcal{J}_{\text{II}}$  and from Ampère's law

$$H(r) = \frac{4R^2\rho(0)\mathcal{J}_{\text{II}}(1 + \cos x)}{\pi} = \frac{1}{2}H(0)(1 + \cos x) \quad (47)$$

where  $x = \pi r/R$  and  $H(R) = 0$ . The dimensionless combination

$$\hat{\mathcal{J}}_{\text{II}} \equiv \frac{4R^2\rho(0)\mathcal{J}_{\text{II}}}{\pi H(0)} = \frac{1}{2}; \quad (48)$$

moreover

$$b = \frac{d \ln H}{d \ln \rho} = \frac{x \sin x}{(1 + \cos x)(1 - x \cot x)} \quad (49)$$

varies monotonically between  $b = 3/2$  and  $b = 2$  from the center of the star to the surface. Although this model is not truly physical because  $H(\rho) = H(\rho/\rho(0))$  depends on the central density, hence mass, of the star and so involves a density scale that is not the same for all stars,  $3/2 \leq b \leq 2$  is an acceptable range for nuclear equations of state. Moreover, when we consider models with  $H \propto \rho^b$  with realistic values of  $b$ , we shall see that even though  $\hat{\mathcal{J}}(A)$  is no longer constant, its values are close to 0.5 for cases where field lines hit the outer boundary of the core vertically; because field lines are vertical at the equator, they remain close to vertical throughout the core in these cases, as may be seen from Fig. 3.

The interior field must match onto the field in the normal shell. If the transition from superconductor to normal conductor occurs in a transition region of negligible thickness, then the field is dipolar in the shell to a good approximation, and is given by Eq. (31) and Eq. (32). Eq. (32) holds generally for the dipole field within the normal shell; for the toy model  $H_b = \frac{1}{2}H(0)(1 + \cos x_b)$  so

$$\hat{\mathcal{J}}_{\text{shell}} = \frac{1}{2} \left( 1 + \frac{B}{2H_b} \right) = \hat{\mathcal{J}}_{\text{II}} \left( 1 + \frac{B}{2H_b} \right). \quad (50)$$

The core and shell current density parameters are nearly the same in this toy model for  $B/2H_b \ll 1$ . This will also be true for more realistic models, but the difference will be  $\sim 0.1$ , not  $\sim B/H_b$ . For the toy model, the perturbations caused by  $\Delta\hat{\mathcal{J}}(A)$  are very small, since  $\beta(\hat{\mathcal{J}}_{\text{II}} - \hat{\mathcal{J}}_{\text{shell}}) = \frac{1}{2}\beta B\hat{\mathcal{J}}_{\text{II}}/H_b$ , and we shall ignore them; for realistic models, where  $\hat{\mathcal{J}}_{\text{II}} - \hat{\mathcal{J}}_{\text{shell}} \sim 0.1$ , the perturbations are larger,  $\sim 0.1\beta$ .

In general, there will be a contribution to the stellar distortion  $\propto B$ . One reason is that  $H_b \rightarrow H_b + B/2$  in the dipole solution within the shell; thus we substitute  $H_b^2 \rightarrow (H_b + B/2)^2 \simeq H_b^2 + H_b B$  in Eq. (45). There are also contributions from the terms in the solution that are  $\propto B$ . For the toy model with  $\hat{\mathcal{J}}_{\text{II}} = \frac{1}{2} \simeq \hat{\mathcal{J}}_{\text{shell}}$  the extra  $l = 2$  contribution to the driving term is

$$\Delta\mathcal{M}_2(x) = -\frac{\pi H(0)Br_b^2}{24R^2\rho(0)} \begin{cases} (x/x_b)^2 & \text{if } x \leq x_b \\ x_b/x & \text{if } x_b \leq x \leq \pi \end{cases} \quad (51)$$

which implies an additional quadrupole moment

$$\Delta\mathcal{M}_2 = -\frac{H(0)Br_b^2R^2\Delta\mathcal{I}(x_b)}{6\pi GM^2} = -\frac{1.03 \times 10^{-9} H_{b,14}^2 R_{10}^4 \Delta\mathcal{I}(x_b)}{M_{1.4}^2} \frac{B}{H_b} \quad (52)$$

where  $\Delta\mathcal{I}(x_b) = \Delta\mathcal{I}_{\text{II}}(x_b) + \Delta\mathcal{I}_{\text{shell}}(x_b)$  with core and shell contributions

$$\begin{aligned} \Delta\mathcal{I}_{\text{II}}(x_b) &= \frac{2(r_b/R)^2}{1 + \cos x_b} \left[ \left( \frac{15}{x_b^2} - 6 \right) \sin x_b + \left( x_b - \frac{15}{x_b} \right) \cos x_b \right] \\ \Delta\mathcal{I}_{\text{shell}}(x_b) &= \frac{2(r_b/R)^2}{1 + \cos x_b} [-x_b(1 + \cos x_b) + 3 \sin x_b] \end{aligned} \quad (53)$$

respectively. The crust contribution  $\Delta\mathcal{I}_{\text{shell}}(x_b)$  is the same in realistic models. For thin shells,  $\Delta\mathcal{I}_{\text{shell}}(x_b) \simeq 12/\delta_b$  and  $\Delta\mathcal{I}_{\text{shell}}(0.9\pi) = 26.1$ . The core contribution  $\Delta\mathcal{I}_{\text{II}}(x_b)$  will be close to the value in the toy model, with differences arising

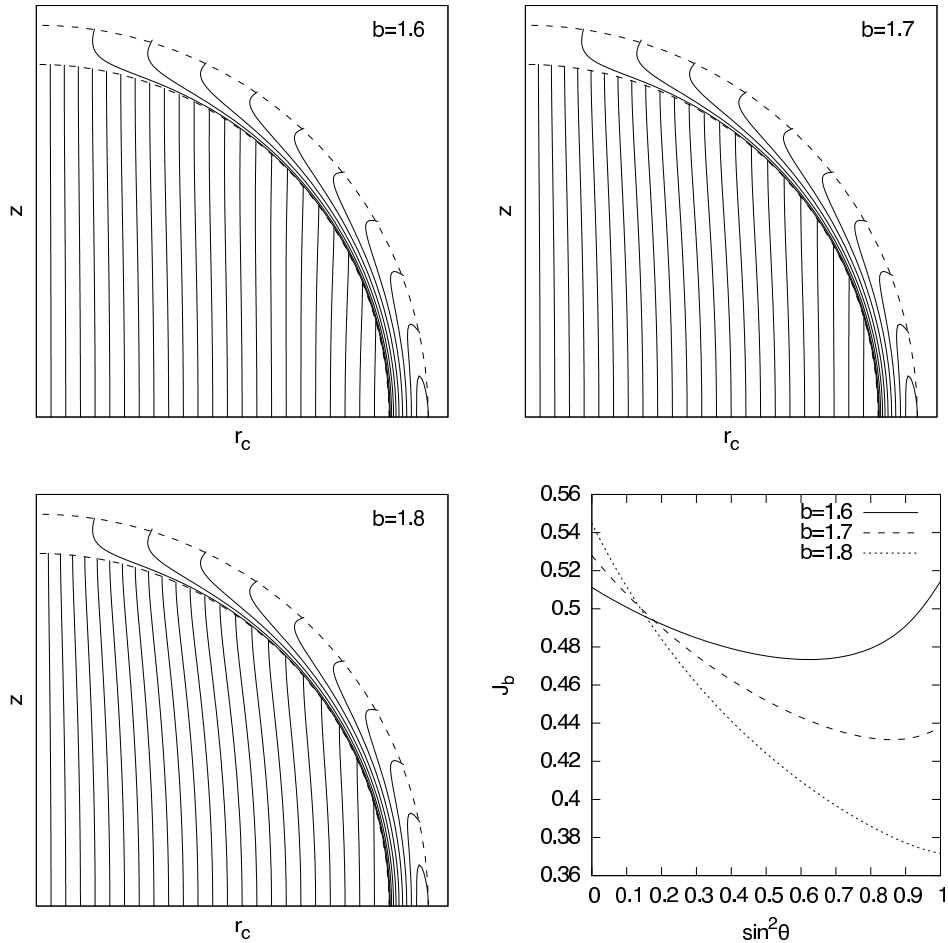


**Figure 3.** Field line configurations assuming  $H(\rho) \propto \rho^b$  with  $b = 1.6, 1.7$  and  $1.8$ . The inner and outer dashed lines show the boundary of the Type II core at  $r = 0.9R$  and the stellar surface at  $r = R$ , respectively, for the stellar magnetic axis in the  $z$  direction. The lower right panel shows the value of the rescaled current parameter  $\hat{J}$  as a function of  $\sin^2 \theta$  along the inner dashed boundary.

because field lines are not strictly vertical, realistically. For thin shells,  $\Delta \mathcal{I}_{\text{II}}(x_b) \simeq (60/\pi - 4\pi)/\delta_b^2 \simeq 6.5/\delta_b^2$  in the toy model and  $\Delta \mathcal{I}_{\text{II}}(0.9\pi) = 35.8$ . Comparing Eq. (52) with Eq. (46) we see that  $|\Delta \mathcal{M}_2| \lesssim (\beta/\epsilon_b)|\mathcal{M}_2|$  characteristically.

## 4 NUMERICAL SOLUTIONS

### 4.1 Field Line Structure

In the strong Type II limit where  $H = H_{c1}(\rho)$  does not depend on  $B$ , we can solve Eq. (17) and Eq. (19) for each magnetic field line individually. Symmetry dictates that field lines be vertical at their equatorial footpoints. For the “most dipolar” solutions that match to a pure dipole field in the normal shell to zeroth order in  $\ell$  and  $\beta$ , we also require that each field line be vertical at  $x_b$ . We can label each field line by its footpoint radius,  $x_0$ . Once we specify  $H(\rho) = H_{c1}(\rho)$  we can find the value of  $\hat{J}(x_0)$  for which these conditions are satisfied. Thus, we determine both the source and the field line shapes that are consistent with our boundary conditions.

In order to choose the function  $H(\rho)$  we fit the values of the proton fraction given in Zuo et al. (2008) to power laws of the baryon density. Writing  $H(\rho) \propto \rho^b$ , we found that  $b \approx 1.6 - 1.8$ . We used the  $N = 1$  polytrope for the mass density profile of the star.

Fig. 3 shows the results for  $b = 1.6, 1.7$  and  $1.8$ . Note that there are two competing features of the solutions:  $\nabla H$  tends to curve the field lines inward, and  $\hat{J}(x_0)$  opposes this trend. The field lines are most nearly vertical throughout the core for  $b = 1.6$ , the smallest value displayed. Even though the field line shapes are not precisely vertical throughout the core, the deviations are relatively small. We have also found the field line solutions for  $b = 1, 1.5$ , and  $2$ ; they are substantially similar to the configurations shown in Fig. 3.

The lower right panel shows the current density parameter  $\hat{J}_b$  as a function of  $\sin^2 \theta$ . This quantity is found by determining  $\hat{J}(x_0)$  for each field line; using the solution for  $\theta(\sigma)$  along the line, we find where it intersects the surface  $x_b$ . Note that our solutions *do not* determine the value of  $A$  for a given field line.

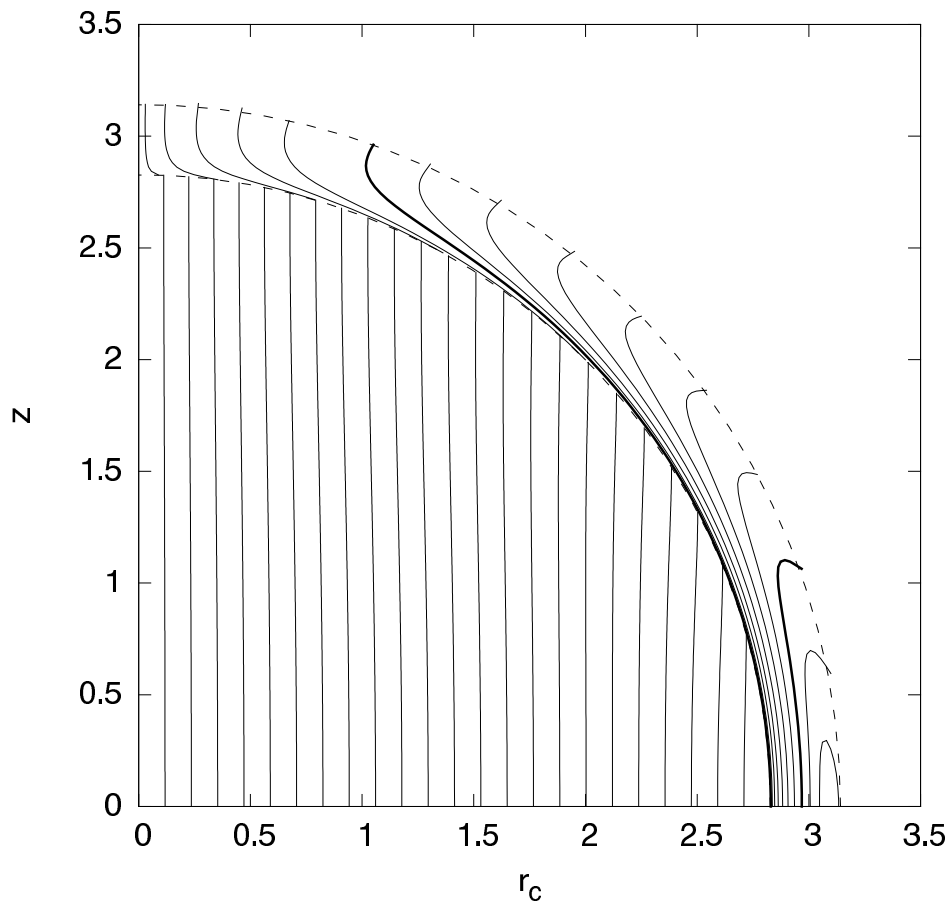


**Figure 4.** Field line configuration in the same layout as in Fig. 3, with nonzero  $B$  field strength at the core boundary. Shown here is the case where  $\beta = 0.1$ , as defined in Eq. (35), and  $b = 1.6$ . Field lines in the shell are computed to lowest order in  $\beta$ ; for corrections see §4.3.

For  $B = 0 = \beta$  and  $\ell = 0$  boundary conditions at the core-shell interface dictate that  $\mathbf{B} = -\hat{\theta}H_b \sin\theta$  at the base of the shell. This means that in this approximation field lines *do not* penetrate from the core to the shell. The solution inside the shell that matches smoothly to a vacuum field is given by Eq. (26). Since there are two boundary conditions at  $x_b$ , the surface boundary condition determines  $\hat{J}_{\text{shell}}$  (Eq. (27)) so the entire solution outside the core not only is determined fully but also depends on  $H_b$ .

Fig. 4 illustrates the field line configuration for  $b = 1.6$  but  $\beta = 0.1$ , to lowest order in  $\beta$ . (Corrections will be considered in §4.3.) In this case, field lines from the core penetrate into the normal shell. The inner thick line shows the bounding field line. It is apparent that field lines hug close to  $x = x_b$  before fanning out into a polar cap whose angular extent is  $\sim \sqrt{\beta}$ . Also shown in this figure is the small region where field lines in the shell are closed: the first open field line has its inner footpoint at  $x \simeq 0.97\pi$ . (This region is also apparent in the  $\beta = 0$  configurations in Fig. 3.) In a fluid shell, this region would be magnetohydrodynamically unstable (Wright 1973; Markey & Tayler 1973) but shear stresses in the normal shell restore stability since the shear modulus  $\mu \gg B^2 \sim 10^{24} B_{12}^2 \text{ g cm}^{-1} \text{ s}^{-2}$  (e.g. Haensel 2001; Horowitz & Kadau 2009; Baiko 2011).

## 4.2 Magnetic Distortion: Mass Quadrupole Moment

In general, there are four contributions to the quadrupolar distortion to linear order in  $B/H_b$ :

$$\mathcal{M}_2 = -10^{-9} H_{b,14}^2 R_{10}^2 M_{1.4}^{-2} \left[ C_1 + (C_2 + C_3 + C_4) \frac{B}{H_b} \right]. \quad (54)$$

The coefficients  $C_1$  and  $C_2$  arise from the shell, and are independent of the core structure; for  $r_b = 0.9R$ ,  $(C_1, C_2) = (+1.58, +28.3)$ . The coefficient  $C_3$  arises from  $\Phi(A)$  and the coefficient  $C_4$  arises from  $B\partial f/\partial\rho$ ; these depend on the structure of the core field: for  $r_b = 0.9R$

$$(C_3, C_4) = \begin{cases} (+30.4, -0.434) & \text{if } b = 1.6 \\ (+35.4, -2.20) & \text{if } b = 1.7 \\ (+40.7, -4.64) & \text{if } b = 1.8 \\ (+36.7, 0) & \text{Toy} \end{cases} \quad (55)$$

$j$	$\hat{\mathcal{J}}_{b,j}$	$Q_j(\ell)/R^{2j-1}\ell\mu$
0	-4.918e-01	1.701e+01
0	0	5.239e-01
1	6.067e-03	-4.999e-01
2	-5.198e-03	2.723e-01
3	1.241e-03	-6.844e-02
4	-3.843e-04	1.973e-02
5	8.526e-05	-3.657e-03

**Table 1.** Values of  $\hat{\mathcal{J}}_{b,j}$  (col. 2),  $Q_j(\ell)/R^{2j}\ell\mu$  (col. 3) for  $j \leq 5$  (col. 1) and  $b = 1.6$  and  $r_b = 0.9R$ . Second line renormalizes  $H_b$  as described in the text.

where in all cases  $C_3 > |C_4|$  because field lines are nearly vertical (exactly vertical in the toy model). Roughly speaking, the coefficient of  $B/H_b$  in Eq. (54) is  $\simeq 60$ , but  $B/H_b \approx 2f(\pi; x_b)R^2\beta/3\pi^2r_b^2 = \beta/14.1$  for  $r_b = 0.9R$ , which mitigates the dependence of  $\mathcal{M}_2$  on  $B$  for small  $\beta$ .

### 4.3 Perturbative Corrections: Nonzero $\ell$ and $\beta$

Table 1 shows the results of computing perturbations resulting from nonzero transition zone thickness using the method developed in Appendix A1. Although the table only contains results for multipoles  $Q_j$  with  $j \leq 5$ , the calculations were performed using  $\hat{\mathcal{J}}_{b,j}$  with  $j \leq 14$ , and therefore determined  $Q_j$  for  $j \leq 14$ . The procedure can be iterated but we did not do so. To obtain these results, we solved Eq. (A12) with  $\Delta A_j(x_b) = 0$ . Appendix B shows that in fact  $\Delta A_j(x_b) \neq 0$ . However, according to Eq. (B7),  $\Delta A_j(x_b)$  is primarily dipolar to  $\mathcal{O}(\ell)$ . This dipolar component as well as the effect of  $\hat{\mathcal{J}}_{b,0}$  may be absorbed into a “renormalized” background solution. The second line in Table 1 tabulates the “extra” change in  $Q_0$  that results when we renormalize in this fashion.

Table 1 shows that the multipole perturbations that result from nonzero  $\ell$  are small but not entirely negligible. For example, the shift in the dipole moment is  $\Delta\mu/\mu = -17.01\ell/R$ ; for  $\ell/R = 0.01$  this is a downward change of about 17%. Since we require  $\Delta A_j(x_b)$  to be relatively small, Eq. (B7) indicates that  $\ell/R \ll B/H_b \sim \beta\epsilon_b$ , so consistency would require somewhat smaller  $-\Delta\mu/\mu$ : shifts are restricted to  $\lesssim$  a few percent. The other multipole moments are smaller by at least a factor of 30.

Implementing the procedure in Appendix A2.1 proved more challenging computationally, particularly for larger values of  $\beta$ , where the various matrices that had to be inverted turned out to be nearly singular. These computational problems did not arise for  $\beta \leq 0.05$ , and for  $10^{-5} \leq \beta \leq 0.05$  we found  $\Delta\mu/\mu \simeq -0.115\beta$  and a RMS change  $\Delta A_{\text{rms}}(R)/A_0(R) \simeq 0.150\beta$  assuming  $b = 1.6$  and  $\epsilon_b = 0.1$ . Thus, although the perturbations are predominantly dipolar, nondipole contributions are only a few times smaller. These results were found using various maximum  $0 \leq j_{\text{in}} \leq 10$  in the expansion for  $\hat{\mathcal{J}}_b(\theta)$ , and various maximum  $10 \leq j_{\text{max}} \leq 14$  in the multipole expansion within the normal shell. Empirically, we found that about 90% of the perturbation arose when we took  $j_{\text{in}} = 0$ , which suggests that the main effect arises from the peculiar shape of the region within the shell occupied by field lines entering from the Type II core; see Fig. 4.

## 5 DISCUSSION AND CONCLUSIONS

In this paper, we developed the formalism for computing the configuration of poloidal magnetic fields inside a neutron star with a strongly Type II superconducting core. Qualitatively, the restriction to hydrostatic balance without “magnetic buoyancy” imposes constraints on the electric current density given by Eq. (10). Because of these constraints, we must determine both the current densities and field line structure at the same time. Within the Type II core, the task is simplified when  $B \ll H$ , for in this limit  $H$  is a function of density, and therefore a function of radius, to lowest order in the magnetic distortion.

The main results of this paper are:

- (i) The Type II core provides an important boundary condition for fields in the normal shell surrounding it; see Eq. (25).
- (ii) If the core is strongly Type II, continuity of the tangential and normal components of magnetic field imply that the field points very nearly along the inner boundary of the normal shell, unless the field just inside the boundary is tuned finely. Thus, generically field lines from the core do not penetrate deep into the normal shell of the star. However, the field strength at the base of the normal shell is  $\sim H_b$  in this case.
- (iii) Substantial currents in the normal shell are required for the field to adjust in strength and direction to conform with vacuum boundary conditions at the radius of the star.
- (iv) In the “most dipolar case” in which the field is vertical at the outer edge of the Type II core, the emerging field is dipolar, with a surface field strength given by Eq. (26).
- (v) If the thickness of the normal shell of the star is  $\epsilon_b R$  with  $\epsilon_b \ll 1$ , the surface field strength for the “most dipolar” case is  $\simeq H_b\epsilon_b/3$ . For typical neutron star parameters Eq. (4) implies a surface field strength  $\simeq 3 \times 10^{12}$  G, which is characteristic of the large population of “normal neutron stars.”

(vi) Magnetic fields induce a quadrupolar distortion of the star  $\mathcal{M}_2 \simeq -10^{-9}$ . The scale of the distortion is set primarily by  $H_b$  for small  $B/H_b$ ; see Eq. (54).

(vii) Perturbations arise from the finite thickness of the transition layer in which the superconductor disappears and from field lines that penetrate from the Type II core to the normal shell. These perturbations are small if  $\ell/\epsilon_b R \ll \beta \ll 1$ , which delineates the domain of validity of our calculations.

Although our calculations assume a star in hydrostatic balance, some of the qualitative features found here would hold for stars that are out of equilibrium as well. For example, in configurations without surface currents, we would still expect field lines to emerge from the core pointing largely along the inner boundary of the normal shell, with a field strength there  $\sim H_b$ . Consequently, we would still expect the emerging field to have a field strength similar to what is found in equilibrium.

Our calculations have employed a very simple equation of state: the  $N = 1$  polytrope. Within the context of this equation of state, if we stipulate that  $\rho_b$  is fixed by microphysics of the phase change from core fluid with free protons to a crystalline crust with protons confined to nuclei, then  $H_b$  will be independent of the stellar mass. However, since  $R$  is fixed for a (Newtonian)  $N = 1$  polytrope the central density is  $\propto M$  and the fractional thickness of the normal shell is  $\propto 1/M$ . Thus, we would expect some variation of the surface magnetic field with stellar mass, but this would only lead to a rather small range of values differing by less than a factor of two.

More realistically, with  $H_b$  fixed the surface field strength will still be  $\propto H_b \epsilon_b$ , but the value of  $\epsilon_b$  and the proportionality constant would depend on details of the equation of state. We expect this to remain so even if the Type II region does not encompass the entire stellar core, as we have assumed here: Type II superconductor with an inner boundary would have different currents but the lower boundary condition on the normal shell is sensitive primarily to  $H_b$ . Nevertheless, very generally we expect that the “most dipolar” case will result in field strengths  $\sim 10^{12}$  G with little variation. This is contrary to observations, which show that even the dipolar field strengths, as indicated by the  $P - \dot{P}$  diagram for radiopulsars (e.g. Lorimer & Kramer 2012), vary over several orders of magnitude.

The obvious solution to this problem is that the magnetic field configurations for many pulsars are very similar to the most dipolar configuration, but that there may be substantial deviations. We envision several reasons for such variation:

- (i) The strong Type II limit fails because  $B \sim H$  in the core. We expect that this is true for magnetars, for example.
- (ii) Failure of the strong Type II limit is an extreme example of a case that is outside the scope of the calculations in this paper. There are configurations with  $B \ll H_b$  that violate our requirements: (a) If  $\epsilon_b^{-1} \gg \beta \gtrsim 1$  field lines impinging from the core affect the surface field non-perturbatively. (b) If  $\beta$  is small enough that  $\ell/R \gtrsim B/H_b \sim \beta \epsilon_b$  then field lines curve significantly within the transition region between the Type II core and normal shell, which would affect their coupling.
- (iii) Toroidal magnetic fields, which were not considered here, can alter the poloidal field configuration even in hydrostatic equilibrium. We will treat this possibility elsewhere. Toroidal fields also mitigate instability. We have seen that there is a region in the normal shell that would be unstable if the normal shell were a pure fluid (see Fig. 4) although in a crystalline crust shear stresses should suffice to ensure stability there. However, the Muzikar-Pethick-Roberts instability in the Type II core (Muzikar & Pethick 1981; Roberts 1981; Akgün & Wasserman 2008) might require toroidal fields to ensure stability.
- (iv) Even if none of the last three caveats holds, so the core is in the strong Type II regime and toroidal fields do not affect the poloidal fields significantly, the requirement that field lines hit the outer boundary of the Type II core vertically that is the basis for the most dipolar configuration is very special. Relaxing it could lead to greater diversity in surface field strengths.

We expect that of these options the last is most important for neutron stars with surface magnetic field strengths substantially below  $10^{12}$  G. The extreme case is when field lines hit the outer boundary of the Type II core radially. The field line configuration within the core is shown in Fig. 1, Panel a. In this extreme, the field remains radial as it enters the normal shell, and is weak in strength,  $\sim B \ll H_b$ . Entering field lines carry current density  $\sim c\rho_b H(0)/\rho(0)R$  with them, and therefore curve downward toward the stellar equator within a short distance of the boundary: crudely the field should penetrate a distance  $\sim B\rho(0)R/\rho_b H(0)$ , which is  $\sim \beta(\rho_b/\rho(0))^{b-1} \ll 1$  times the thickness of the shell. We might then expect that the entering field lines are confined to a small region of the normal shell, and the field strength at the surface could be  $\lesssim B\epsilon_b$ , which may be very small. We will report elsewhere on calculations that employ different boundary conditions at the outer radius of the Type II core.

Even though it relies on special conditions, the “most dipolar” solution reveals that there is a characteristic surface magnetic fields strength that is determined by the nuclear equation of state. Our calculations show that this field strength is  $\sim 10^{12}$  G, reassuringly close to the values deduced for many neutron stars. By relaxing the restrictive boundary conditions underlying the most dipolar solution, it seems plausible that a variety of field strengths may be attained in equilibrium. Field strengths  $\gg 10^{12}$  G or  $\ll 10^{12}$  G may be attained under other restrictive conditions.

## ACKNOWLEDGEMENTS

We thank S. Lander and A. Sedrakian for helpful correspondence. This research was supported in part by NSF grant AST-0606710, NSF grant PHY11-25915, by a fellowship from the NASA/New York Space Grant Consortium and by the College of Arts and Sciences, Cornell University.

**REFERENCES**

- Akgün T., 2007, PhD thesis, Cornell University  
Akgün T., Wasserman I., 2008, MNRAS, 383, 1551  
Alpar M. A., Langer S. A., Sauls J. A., 1984, ApJ, 282, 533  
Andersson N., Comer G. L., Glampedakis K., 2005, Nuclear Physics A, 763, 212  
Andreev A. F., Bashkin E. P., 1975, Soviet Journal of Experimental and Theoretical Physics, 42, 164  
Baiko D. A., 2011, MNRAS, 416, 22  
Baym G., Bethe H. A., Pethick C. J., 1971, Nuclear Physics A, 175, 225  
Baym G., Pethick C., Pines D., 1969, Nature, 224, 673  
Blandford R. D., Applegate J. H., Hernquist L., 1983, MNRAS, 204, 1025  
Demorest P. B., Pennucci T., Ransom S. M., Roberts M. S. E., Hessels J. W. T., 2010, Nature, 467, 1081  
Easson I., Pethick C. J., 1977, Phys. Rev. D, 16, 275  
Flowers E., Ruderman M., Sutherland P., 1976, ApJ, 205, 541  
Haensel P., 2001, in Blaschke D., Glendenning N. K., Sedrakian A., eds, Physics of Neutron Star Interiors Vol. 578 of Lecture Notes in Physics, Berlin Springer Verlag, Neutron Star Crusts. p. 127  
Hebel K., Schwenk A., Friman B., 2007, Physics Letters B, 648, 176  
Horowitz C. J., Kadau K., 2009, Physical Review Letters, 102, 191102  
Lander S. K., 2013, Physical Review Letters, 110, 071101  
Lander S. K., Andersson N., Glampedakis K., 2012, MNRAS, 419, 732  
Lorimer D. R., Kramer M., 2012, Handbook of Pulsar Astronomy. Cambridge University Press  
Markey P., Tayler R. J., 1973, MNRAS, 163, 77  
Mastrano A., Melatos A., Reisenegger A., Akgün T., 2011, MNRAS, 417, 2288  
Monaghan J. J., 1965, MNRAS, 131, 105  
Muzikar P., Pethick C. J., 1981, Phys. Rev. B, 24, 2533  
Page D., Prakash M., Lattimer J. M., Steiner A. W., 2011, Phys. Rev. Lett., 106, 081101  
Pons J. A., Miralles J. A., Geppert U., 2009, A&A, 496, 207  
Prendergast K. H., 1956, ApJ, 123, 498  
Roberts P. H., 1981, The Quarterly Journal of Mechanics and Applied Mathematics, 34, 327  
Sedrakian A. D., Sedrakian D. M., 1995, ApJ, 447, 305  
Shternin P. S., Yakovlev D. G., Heinke C. O., Ho W. C. G., Patnaude D. J., 2011, MNRAS, 412, L108  
Wentzel D. G., 1961, ApJ, 133, 170  
Woltjer L., 1960, ApJ, 131, 227  
Wright G. A. E., 1973, MNRAS, 162, 339  
Zuo W., 2012, ArXiv e-prints  
Zuo W., Cui C. X., Lombardo U., Schulze H.-J., 2008, Phys. Rev. C, 78, 015805  
Zuo W., Li Z., Lu G., Li J., Scheid W., Lombardo U., Schulze H.-J., Shen C., 2004, Physics Letters B, 595, 44

**APPENDIX A: PERTURBATION SOLUTIONS**

We begin with a zeroth order solution,  $A_0(x, \theta)$ , that corresponds to a given  $\hat{\mathcal{J}}_{\text{shell}}(A)$ ; we use Eq. (26). Perturbations distort the solution to

$$A(x, \theta) = A_0(x, \theta) + \sin \theta \sum_{J=0}^{\infty} \Delta A_J(x) P_{2J+1}^1(\cos \theta). \quad (\text{A1})$$

The perturbed solution corresponds to  $\hat{\mathcal{J}}(A) = \hat{\mathcal{J}}_{\text{shell}} + \Delta \hat{\mathcal{J}}(A)$ , where  $\Delta \hat{\mathcal{J}}(A)$  must be determined along with the perturbed field solution. To do this, we begin by choosing a functional form for  $\Delta \hat{\mathcal{J}}(A)$  which will necessarily involve unknown parameters to be determined. Since  $A \approx A_0$  by assumption, we substitute  $\Delta \hat{\mathcal{J}}(A) \approx \Delta \hat{\mathcal{J}}(A_0)$  to find the perturbed field; because  $A_0$  is known we may expand

$$\sin \theta \Delta \hat{\mathcal{J}}(A_0) = \sum_{j=0}^{\infty} S_j(x) P_{2j+1}^1(\cos \theta) \quad (\text{A2})$$

to get the equation

$$\frac{d^2 \Delta A_j}{dx^2} - \frac{(2j+1)(2j+2) \Delta A_j}{x^2} = - \frac{H(0) R^2 x \sin x S_j(x)}{\pi^2}, \quad (\text{A3})$$

which, with the boundary condition  $x d \Delta A_j / dx + (2j+1) \Delta A_j = 0$ , has the solution

$$\Delta A_j(x) = \frac{\Delta A_j(x_b) x_b^{2j+1}}{x^{2j+1}} + \frac{H(0) R^2}{(4j+3) \pi^2} \left[ x^{2j+2} \int_x^\pi \frac{dx' \sin x' S_j(x')}{(x')^{2j}} \right]$$

$$-\frac{x_b^{4j+3}}{x_b^{2j+1}} \int_{x_b}^{\pi} \frac{dx' \sin x' S_j(x')}{(x')^{2j}} + \frac{1}{x_b^{2j+1}} \int_{x_b}^x dx' (x')^{2j+3} \sin x' S_j(x') \Big]. \quad (\text{A4})$$

Differentiating Eq. (A4) and evaluating at  $x_b$  implies

$$-\frac{R^2 \Delta B_{\theta,j}(x_b)}{\pi^2} = \left( \frac{1}{x} \frac{d\Delta A_j}{dx} \right)_{x_b} = -\frac{(2j+1)\Delta A_j(x_b)}{x_b^2} + \frac{H(0)R^2 x_b^{2j}}{\pi^2} \int_{x_b}^{\pi} \frac{dx' \sin x' S_j(x')}{(x')^{2j}} \quad (\text{A5})$$

where the perturbed field tangential to the boundary at  $x_b$  is

$$\Delta B_{\theta}(x_b, \theta) = \sum_{j=0}^{\infty} \Delta B_{\theta,j}(x_b) P_{2j+1}^1(\cos \theta). \quad (\text{A6})$$

Eq. (A5), given Eq. (A6), is used to determine the unknown parameters of the source term,  $\Delta \hat{\mathcal{J}}(A)$ . Once these parameters have been found, Eq. (A4) evaluated at  $x = \pi$  determines the multipole moments  $Q_j = \Delta A_j(\pi) R^{2j+1}$ :

$$Q_j = \Delta A_j(x_b) r_b^{2j+1} + \frac{H(0)r_b^{2j+3}}{4j+3} \int_{x_b}^{\pi} dx' \sin x' S_j(x') \left[ \left( \frac{x'}{x_b} \right)^{2j+3} - \left( \frac{x_b}{x'} \right)^{2j} \right]. \quad (\text{A7})$$

Non-trivial perturbations will always engender multipole fields at the surface.

### A1 Surface Currents from Transition Layer

We write the zeroth order solution as  $A_0 = A_s \tilde{f}(x; x_b) \sin^2 \theta$ , where  $A_s = F_0(\pi)$  so  $\tilde{f}(\pi; x_b) = 1$ , and expand

$$\Delta \hat{\mathcal{J}}(A) = \sum_{j=0}^{j_{\max}} \Delta \hat{\mathcal{J}}_n \left( \frac{A}{A_s} \right)^n \approx \sum_{J=0}^{j_{\max}} \Delta \hat{\mathcal{J}}_n (\sin \theta)^{2n} [\tilde{f}(x; x_b)]^n \quad (\text{A8})$$

where we substituted  $A \approx A_0$ ; then

$$S_j(x) = \sum_{n=j}^{j_{\max}} \frac{N_{nj} \Delta \hat{\mathcal{J}}_n [\tilde{f}(x; x_b)]^n}{N_j}, \quad (\text{A9})$$

$$N_{nj} = \frac{2\pi \Gamma(n+2) \Gamma(n+1)}{\Gamma(n+j+\frac{5}{2}) \Gamma(n-j+1) \Gamma(j+1) \Gamma(-j-\frac{1}{2})}$$

For sufficiently small transition region thickness  $\ell$  the jump condition from Type II core to normal shell is given by Eq. (29), and therefore

$$\Delta B(x_b, \theta) = \frac{\pi \ell \hat{\mathcal{J}}_b(\theta) H(0) \sin x_b \sin \theta}{R} \quad (\text{A10})$$

where  $\hat{\mathcal{J}}_b(\theta)$  is the current density parameter at the outer edge of the Type II core, which we compute for each field line; then with

$$\sin \theta \hat{\mathcal{J}}_b(\theta) = \sum_{j=0}^{\infty} \hat{\mathcal{J}}_{b,j} P_{2j+1}^1(\cos \theta) \quad (\text{A11})$$

Eq. (A5) becomes

$$-\frac{\pi \ell \hat{\mathcal{J}}_{b,j} \sin x_b}{R} + \frac{(2j+1)\Delta A_j(x_b)}{H(0)r_b^2} = \sum_{n=j}^{j_{\max}} \frac{N_{nj} \Delta \hat{\mathcal{J}}_n}{N_j} \int_{x_b}^{\pi} \frac{dx \sin x [\tilde{f}(x; x_b)]^n}{(x/x_b)^{2j}}, \quad (\text{A12})$$

which is a linear equation for the  $\Delta \hat{\mathcal{J}}_n$ . The multipole moments are then found by combining Eqs. (A7), (A9) and the solution of Eq. (A12).

### A2 Field Lines Poking in from the Core

We do not know  $A(x_b, \theta)$  *a priori*. In the strong Type II core, field lines are labelled by their foot points  $x_0$ , and our solutions determine (i) the value of  $\theta$  where they hit the boundary and (ii) the value of  $\hat{\mathcal{J}}_b(\theta)$  there, subject to whatever constraint we impose on the solution, such as for the ‘‘most dipolar’’ solution. We need  $A(x_b, \theta)$  in order to map  $\hat{\mathcal{J}}_b(\theta) \rightarrow \hat{\mathcal{J}}_{\text{core}}(A)$ , which is needed to determine the effect of impinging field lines on the normal shell solution.

$$A2.1 \quad A(x_b, \theta) = \frac{1}{2} Br_b^2 \sin^2 \theta$$

In this case, the background solution is Eq. (31) with current parameter Eq. (32). We take  $\Delta B_j(x_b) = 0 = \Delta A_j(x_b)$ .

A key feature of this background solution is that field lines from the Type II core penetrate into the normal shell, bringing along the currents  $\hat{\mathcal{J}}_{\text{II}}(A) = \hat{\mathcal{J}}_b(\theta(A))$  associated with them, where  $\theta(A) = \sin^{-1}(\sqrt{2A/Br_b^2})$ . Defining  $\Delta \hat{\mathcal{J}}_{\text{II}}(A) = \hat{\mathcal{J}}_{\text{II}}(A) - \hat{\mathcal{J}}_{\text{shell}}(B)$  we have

$$\begin{aligned} \Delta \hat{\mathcal{J}}(A) &= \Delta \hat{\mathcal{J}}_{\text{II}}(A) \Theta\left(\frac{1}{2} Br_b^2 - A\right) + \Delta \hat{\mathcal{J}}_{\text{shell}}(A) \Theta\left(A - \frac{1}{2} Br_b^2\right) \\ &\approx \Delta \hat{\mathcal{J}}(A_0) \Theta(\theta_{\text{II}}(x) - \theta) + \Delta \hat{\mathcal{J}}_{\text{shell}}(A_0) \Theta(\theta - \theta_{\text{II}}(x)), \end{aligned} \quad (\text{A13})$$

where the second line assumes  $A \approx A_0$ , and

$$\begin{aligned} S_j(x) &= \frac{2}{N_j} \left[ \int_{\cos \theta_{\text{II}}(x)}^1 d\mu \sqrt{1 - \mu^2} \Delta \hat{\mathcal{J}}_{\text{II}}(A_0) P_{2j+1}^1(\mu) \right. \\ &\quad \left. + \int_0^{\cos \theta_{\text{II}}(x)} d\mu \sqrt{1 - \mu^2} \Delta \hat{\mathcal{J}}_{\text{shell}}(A_0) P_{2j+1}^1(\mu) \right]. \end{aligned} \quad (\text{A14})$$

Generically, the first term in Eq. (A14) is  $\mathcal{O}(1)$  for  $x - x_b \lesssim \beta \epsilon_b$  and is  $\mathcal{O}(\beta^2)$  for  $x - x_b \sim \epsilon_b$ . To find  $\Delta \hat{\mathcal{J}}_{\text{shell}}(A)$  we must first specify its functional form and then determine the associated parameters from Eq. (A5) with  $\Delta B_{\theta,j}(x_b) = 0$ ; the generic scalings suggest that  $\Delta \hat{\mathcal{J}}_{\text{shell}}(A) = \mathcal{O}(\beta)$ . If we expand

$$\Delta \hat{\mathcal{J}}_{\text{II}} = \sum_{n=0}^{j_{\text{max}}} \Delta \hat{\mathcal{J}}_{n,\text{II}} \sin^{2n} \theta \quad (\text{A15})$$

on  $x_b$ , with known coefficients  $\{\Delta \hat{\mathcal{J}}_{n,\text{II}}\}$  and  $\Delta \hat{\mathcal{J}}_{\text{shell}}(A)$  as in Eq. (A8) with *unknown* coefficients  $\{\Delta \hat{\mathcal{J}}_{n,\text{shell}}\}$

$$\begin{aligned} S_j(x) &= \frac{1}{N_j} \sum_{n=0}^{j_{\text{max}}} \left\{ \mathcal{N}_{n,j}(x) \Delta \hat{\mathcal{J}}_{n,\text{II}} + \left[ \frac{N_{nj} [\beta x_b/x + \tilde{f}(x; x_b)]^n - \beta^n \mathcal{N}_{n,j}(x)}{(\beta r_b/R + 1)^n} \right] \Delta \hat{\mathcal{J}}_{n,\text{shell}} \right\} \\ \mathcal{N}_{n,j}(x) &\equiv \frac{2}{\sin^{2n} \theta_{\text{II}}(x)} \int_{\cos \theta_{\text{II}}(x)}^1 d\mu (1 - \mu^2)^{n+1/2} P_{2j+1}^1(\mu); \end{aligned} \quad (\text{A16})$$

although  $N_{n,j} = 0$  for  $j > n$ ,  $\mathcal{N}_{n,j}(x) \neq 0$  in general. The  $\{\Delta \hat{\mathcal{J}}_{n,\text{shell}}\}$  are the solution of

$$\begin{aligned} 0 &= \sum_{n=0}^{j_{\text{max}}} \left( \Delta \hat{\mathcal{J}}_{n,\text{II}} - \frac{\beta^n \Delta \hat{\mathcal{J}}_{n,\text{shell}}}{(\beta r_b/R + 1)^n} \right) \int_{x_b}^{\pi} \frac{dx \sin x \mathcal{N}_{n,j}(x)}{(x/x_b)^{2j}} \\ &\quad + \sum_{n=j}^{j_{\text{max}}} N_{nj} \Delta \hat{\mathcal{J}}_{n,\text{shell}} \int_{x_b}^{\pi} \frac{dx \sin x [\beta x_b/x + \tilde{f}(x; x_b)]^n}{(x/x_b)^{2j} (\beta r_b/R + 1)^n}. \end{aligned} \quad (\text{A17})$$

## A2.2 General $A(x_b, \theta)$

We can incorporate more complicated  $A(x_b, \theta)$ ; let

$$A(x_b, \theta) = \frac{1}{2} Br_b^2 \left[ \sin^2 \theta + \sin \theta \sum_{j=1}^{\infty} a_j P_{2j+1}^1(\cos \theta) \right]; \quad (\text{A18})$$

the coefficients  $\{a_j\}$  may be derived from a given  $A(x_b, \theta)$  via inversion. Eq. (A18) implies a different mapping  $\theta(A)$  on  $x_b$ , hence a different form of  $\hat{\mathcal{J}}_{\text{II}}(A)$  for impinging field lines. With Eq. (A18), the background solution is multipolar. The  $j = 0$  component is Eq. (31) but the other multipoles are generically

$$\begin{aligned} A_j(x) &= \frac{Br_b^2 a_j x_b^{2j+1}}{2x^{2j+1}} + \frac{H(0)R^2}{(4j+3)\pi^2} \left[ x^{2j+2} \int_x^{\pi} \frac{dx' \sin x' S_j^{(0)}(x')}{(x')^{2j}} \right. \\ &\quad \left. - \frac{x_b^{4j+3}}{x^{2j+1}} \int_{x_b}^{\pi} \frac{dx' \sin x' S_j^{(0)}(x')}{(x')^{2j}} + \frac{1}{x^{2j+1}} \int_{x_b}^x dx' (x')^{2j+3} S_j^{(0)}(x') \right]. \end{aligned} \quad (\text{A19})$$

The current density in this model is  $\hat{\mathcal{J}}_{\text{shell}} + \hat{\mathcal{J}}^{(0)}(A)$ , where  $\hat{\mathcal{J}}^{(0)}(A)$  must be determined. Because the impinging fields are weak compared with  $H_b$ , we can determine the currents perturbatively via the analogues of Eqs. (A2), (A8) and (A9), plus the analogue of Eq. (A5) with the condition  $\Delta B_j(x_b) = 0$ .



Once the full background solution has been found, the boundary of the region to which impinging field lines are confined may be determined. We can then proceed as in §A2.1 to find the perturbation to the background solution. Eq. (A18) implies a total flux  $A(x_b, \pi/2)$  through the upper hemisphere. Consistency of the perturbation theory requires  $A(x_b, \pi/2) \ll H_b R^2 \epsilon_b$ .

## APPENDIX B: THE THIN SHELL APPROXIMATION FOR THE TRANSITION LAYER

The proton density plummets in a thin layer that extends from  $r = r_b$  to  $r = r_b + \ell$ ; let  $r = r_b + \ell s$ . As  $n_p$  falls, so does  $\Delta_p$  and the superconductor disappears. For small enough  $p_{F,p}$ , nonzero temperature will matter: for  $\Delta_p \sim T$ , the superconductor may first become Type I before disappearing entirely at  $p_{F,p} \neq 0$ . Our treatment here assumes that  $T \neq 0$  is only important in a very thin subdomain of the transition layer that has little effect on the magnetic field. With  $\Delta_p \propto p_{F,p}^2$  at small  $p_{F,p}$  for  $T = 0$  (Andersson et al. 2005, e.g.) Eq. (1) implies  $\kappa \propto p_{F,p}^{-1/2}$ , so the superconductor remains Type II. However, as  $k_L$  shrinks interactions among field lines become increasingly important; if  $H_{c1}(\rho) = H_{c1}(s)$  within the layer, then the magnetic field strength is

$$H = H_{c1}(s) + Bf \left( \sqrt{\frac{H_{c1}(s)}{B}} \right) \quad (\text{B1})$$

where  $H_{c1}(s)$  is given by Eq. (3) and  $f(0) = 1$  and  $f(z) \rightarrow 0$  exponentially as  $z \rightarrow \infty$ . Ampère's law is

$$\frac{\pi \ell \sin x_b H(0) \hat{\mathcal{J}}(A) \sin \theta}{R} = \frac{\partial H_\theta}{\partial s} + \frac{\ell}{r} \left( H_\theta - \frac{\partial H_r}{\partial \theta} \right); \quad (\text{B2})$$

if we assume that field lines do not rotate significantly, so that we can identify  $A$  with  $\theta$ , and only retain the lowest order in  $\ell$ , Eq. (B2) implies

$$-H_\theta(s, \theta) \simeq \left[ H_b - \frac{\pi \ell s \sin x_b H(0) \hat{\mathcal{J}}(A)}{R} \right] \sin \theta. \quad (\text{B3})$$

The magnetic induction field is

$$\mathbf{B} = -\frac{\hat{\theta}}{\ell r \sin \theta} \frac{\partial A}{\partial s} + \frac{\hat{r}}{r^2 \sin \theta} \frac{\partial A}{\partial \theta}; \quad (\text{B4})$$

in the thin layer approximation we assume that  $B_r$  remains constant and therefore  $B_\theta = \pm \sqrt{1 - B_r^2/B^2}$ . We assume that  $H_\theta$  (and  $B_\theta$ ) remain in the  $-\hat{\theta}$  direction, so

$$\left[ H_b - \frac{\pi \ell s \sin x_b H(0) \hat{\mathcal{J}}(A)}{R} \right] \sin \theta \simeq \sqrt{1 - \frac{B_r^2}{B^2}} \left[ H_{c1}(s) + Bf \left( \sqrt{\frac{H_{c1}(s)}{B}} \right) \right], \quad (\text{B5})$$

which is an algebraic equation for  $B$ . Once  $B$  is found from Eq. (B5), we can solve for the change in  $A$ :

$$\frac{\partial A}{\partial s} \simeq \ell r_b \sin \theta \sqrt{B^2 - B_r^2}. \quad (\text{B6})$$

Ultimately,  $B$  approaches Eq. (B3), hence the change in  $A(s, \theta)$  across the layer is

$$\Delta A(\theta) = A(1, \theta) - A(0, \theta) \simeq \ell r_b \sin^2 \theta \left[ H_b - \frac{\pi \ell \sin x_b H(0) \hat{\mathcal{J}}(A)}{2R} \right]. \quad (\text{B7})$$

Eq. (B7) shows that  $\Delta A(\theta)$  is relatively small provided that  $\ell H_b / B r_b \ll 1$ .